Published in final edited form as:
Geophys Res Lett. 2019 May 28; 46(10): 5092–5099. doi:10.1029/2018GL081727.

How much of the sediment in Gale crater's central mound was fluvially transported?

Bradley J. Thomson[1], **Debra L. Buczkowski**[2], **Larry S. Crumpler**[3], **Kimberly D. Seelos**[2], **Caleb I. Fassett**[4]

[1]Department of Earth and Planetary Sciences, University of Tennessee, Knoxville, Tennessee, USA

[2]Johns Hopkins University Applied Physics Lab, Laurel, Maryland, USA

[3]New Mexico Museum of Natural History and Science, Albuquerque, New Mexico, USA

[4]NASA Marshall Spaceflight Center, Huntsville, Alabama, USA

Abstract

The origin of the sedimentary mound within Gale crater, the landing site for the Mars Science Laboratory rover *Curiosity*, remains enigmatic. Here we examine the total potential contribution of fluvial material by conducting a volume-based analysis. On the basis of these results, the mound can be divided into three zones: a lower, intermediate, and upper zone. The top boundary of the lowermost zone is defined by maximal contribution of water-lain sediments, which are ~13 to 20% of the total mound volume. The upper zone is defined by the elevation of the unbreached rim to the north (−2.46 km); sediments above this elevation cannot have been emplaced by flowing water. These volume balance calculations indicate that mechanisms other than flowing water are required to account for the overwhelming majority of the sediments transported into Gale crater. The most likely candidate process is settling from eolian suspension.

INTRODUCTION

The 154-km-diameter impact crater Gale was selected as the landing site for the Mars Science Laboratory (MSL) rover *Curiosity* in part because it presented an opportunity to explore the large central mound (Aeolis Mons, informally known as Mt. Sharp) (e.g., Grant et al., 2011; Golombek et al., 2012). Although there is clear evidence that the mound is sedimentary in origin, there remains uncertainty about the nature of the medium that transported and deposited those sediments, particularly whether the dominant transport agent was wind or water. A lacustrine origin was posited on the basis of observed channels and scarps interpreted as wave-cut terraces (Cabrol et al., 1999; Malin and Edgett, 2000). In contrast, an eolian-dominated formation scenario has been proposed on the basis of the inferred friability of material and lack of boulders (Irwin et al., 2004; Irwin et al., 2005) as well as outward-dipping bedding orientations (Kite et al., 2013). Results from the *Curiosity* rover indicate evidence for fluvial deposition of sediments on the crater floor (Williams et

Corresponding author: Bradley J. Thomson, bthom@utk.edu, Office phone: 865.974.2699.

al., 2013; Grotzinger et al., 2014; Vaniman et al., 2014) and lower mound (e.g., Grotzinger et al., 2015; Fraeman et al., 2016; Fedo et al., 2017; Hurowitz et al., 2017; Rampe et al., 2017). But how much sediment in the central mound could have been contributed by fluvial processes? Here, we address this question with a mass-balance-type approach to compare the volume of the mound with the volume eroded from the catchment area by flowing water (Fig. 1). Specifically, we perform a source-to-sink analysis of the fluvially-transported sediment that was contributed to Gale crater. The ultimate source of fluvial sediment is the erosion of terrain within the catchment area.

On Mars, numerous authors have used a morphometric approach to infer the former flux of water in now-dry channels (e.g., Moore et al., 2003; Fassett and Head, 2005; Irwin et al., 2005; Burr et al., 2010), or estimate discharge from the volume of terminal deposits (e.g., Williams and Malin, 2008). Here, we consider two potential scenarios: one based on the current, modern topography, and another based on inferred paleotopograhy. The first scenario entails minimal assumed parameters and uses an estimate of the total eroded volume from the watershed area as a measure of the sediment supply. This approach is conceptually similar to the sediment budget analyses applied to catchment-fan systems where the volume of depositional fans is compared to the volume of inferred erosion in the catchment area (e.g., Jolivet et al., 2014; Palucis et al., 2014). In the second scenario, antecedent topography inferred from rover observation is included (e.g., Grotzinger et al., 2015).

METHODS

We used topography from the Mars Orbital Laser Altimeter (MOLA) instrument (Smith et al., 1999) and digital elevation models (DEMs) derived from High Resolution Stereo Camera (HRSC) images (Neukum and Jaumann, 2004) given in Fig. 1 (see also Table S1). As is evident in Fig. 1, only a portion of the exterior valley networks mapped by Hynek et al. (2010) lie within the boundaries of the HRSC DEMs. This subset of valley networks was measured and used to define median valley dimensions for the remainder of the contributing networks. Further details and uncertainty analyses are provided in the supplementary on-line materials (SOM) section.

MOUND VOLUME

The current mound volume was determined by measuring the difference in elevation between the mound surface and the inferred basal level, taken to be approximately −4.5 km in elevation. The resulting mound volume is $9.4\pm0.1\times10^3$ km^3. Following previous precedent (e.g., Grotzigner et al., 2015 SOM), we assume that the density of the eroded and deposited material is the same such that they can be directly compared. Volume changes due to the alteration of primary minerals are also not considered; the precipitation of secondary mineral phases in pore space is assumed to have no effect on the volume analysis considered here as it is inferred to be an isovolume process.

For context, this volume of sediment is significantly larger than the Eberswalde fan deposit (6–30 km^3, e.g., Irwin et al., 2015), though smaller than the 1.5×10^4 km^3 layered mesa

within the comparably-sized Henry crater (167.6 km in diameter) (Malin and Edgett, 2000). As discussed in the Supplementary Material, there is some uncertainty in the mound volume that results from the assumed base level and presence of a central peak (e.g., Gabasova and Kite, 2018). If one assumed the base is an inclined plane, for example, the mound volume would be reduced by one-third (i.e., to 6.1×10^{3} km^3). In the second scenario considered here, the volume of the mound is inferred to have been ~1.8×10^{4} km^3, which is roughly twice its present volume (see SOM and Grotzinger et al., 2015).

FLUVIAL ERODED SEDIMENT VOLUME

There are three components to consider in estimating the volume of sediment mobilized by water: the network of small interior channels, the valley network and large entrance breach in the south rim of Gale, and the eroded volume due to overland (i.e., non-channelized) flow.

Small Internal Channels

Gale crater exhibits numerous inward-draining channels but no outlet; evidence suggests it once hosted a lake (e.g., Grotzinger et al., 2015; Palucis et al., 2016), but it remained topographically closed. Numerous small inward-draining channels have been recognized, including 328 interior channel segments and 179 inverted channel segments (Le Deit et al., 2013), which have a total length of 1863 km (Fig. S1). Individual channel segments are typically 100–300 m in width and extend from a few km up to 35 km in length from the rim down to the crater floor. The lower portions of some of these channels stand in positive relief, indicating that a cementing agent has armored these former watercourses to form linear mesas due to later differential erosion (e.g., Pain et al., 2007). In prior measurements of terrestrial and martian inverted channels, the relative uniformity of inverted channel widths has been taken as evidence that these are approximately equal to the original widths of the channel fill deposits (Harris, 1980; Williams et al., 2009; Burr et al., 2010). Therefore, we estimate the total volume of missing material by summing the lengths of small negative-relief channels and valleys, adding the lengths of positive-relief inverted channels, and multiplying the total length by the typical third-order channel cross-sectional area (Table S3), to obtain a volume of roughly 200 km^3 of sediment. For reference, the estimated volume of material removed due to channel incision in Peace Vallis is 0.8 km^3, which is roughly equivalent to the volume of the Peace Vallis fan (0.9 km^3) (Palucis et al., 2014). In the second scenario considered here that includes potential antecedent topography, early crater wall rim erosion is inferred to have contributed a vertical thickness of 0.5 to 0.6 km of material (after Grotzinger et al., 2015) that is deposited over the crater floor (see SOM for further details).

Valley Network System

Within the 1.20×10^{5} km^2 watershed of Gale, 528 valley network segments have been identified (Hynek et al., 2010) and remapped using updated THEMIS mosaics (see SOM; Edwards et al., 2011; Fergason et al., 2013). Our goal is to quantify the eroded valley volume in order to bound the volume of sediment potentially available as Gale infill. We extracted topographic profiles orthogonal to the local downstream direction in order to measure 2D cross-sectional area. Fig. 2 gives a location plot of the 96 profiles (3 to 4

profiles per segment) with markers sized by cross-sectional area. Each valley network segment was assigned a stream order (Strahler, 1957).

For each segment, the eroded volume was determined by multiplying the cross-sectional area against the segment's length. This calculation yields a volume of 109.5 km^3 for the 434 km in the portion of the network included in HRSC DEM h1960_0000. As this represents only about 8% of the total length of the system of 5392 km, we grouped the area measurements by stream order to estimate the length-weighted median for each stream order (Table S3). Multiplying these areas by the total length of a given stream order yields a total cumulative volume of $8.1 \pm 12 \times l0^2$ km^3.

The confluence of the valley network system exterior to Gale is a single large channel, Farah Vallis, that incises the crater's southwest rim (Greeley and Guest, 1987). Farah Vallis has a morphology consistent with other V-shaped martian valley networks (Williams and Phillips, 2001) and is a few km wide and ~100 m deep. The upstream morphology of Farah Vallis is partly buried by Gale ejecta, suggesting that the Gale impact disrupted it while it was active (Irwin et al., 2005),. If a significant fraction of the fluvial erosion occurred before the Gale impact, this would reduce our estimate of the sediment transported into Gale as this sediment would not be available for mound construction. In a similar manner, the routing of the valley network through a partially-filled, 46-km diameter crater (unnamed crater 'A' in Fig. 1) may also have reduced the sediment delivered to Gale (Irwin et al., 2005; Ehlmann and Buz, 2015), but the exact amount of this reduction depends on the timing of flow through the network. Since there is wide uncertainty in determining the magnitude of these effects, we took no further corrective action other than noting that our fluvially transported sediment volume estimate is at the upper end of the range of plausible values.

Overland Flow

In addition to channelized flow, landscape denudation in overland or non-channelized flow must also be considered. To the south, the 120,000 km^2 Gale watershed terminates against the northern rim of the Herschel crater (Fig. 1). Average landscape denudation of 75 m throughout the watershed would yield a volume of sediment that matches the mound volume. However, while such a value might be plausible during the intense erosion in the Early Noachian (Hynek and Phillips, 2001), it is unreasonably high after this time, at least for most places on Mars. Estimates of post-Middle Noachian erosion rates are more than an order of magnitude lower (e.g., Golombek et al., 2006; Matsubara et al., 2018). For example, ~2 m of denudation was inferred in Milna crater watershed in the Margaritifer Sinus Quadrangle during a similar period of time (Buhler et al., 2014). We adopt this value as a representative erosion rate for this time period in Gale, yielding $\sim 2.4 \times 10^2$ km^3 of sediment from the Gale watershed. We acknowledge, however, that erosion rates on Mars vary widely in space and time. But even this value is likely an overestimate for denudation relevant to Gale given the minimal contribution of non-channelized erosion to the Peace Vallis fan (~12% of the channelized eroded volume) estimated previously (Palucis et al., 2014). Additionally, the presence of relatively unmodified Gale ejecta partially blanketing the valley network draining into Gale (Irwin et al., 2005) constrains the volume of material moved by overland flow to be minimal.

DISCUSSION

Based on the current topography, the total volume of material moved by flowing water into Gale is at most ~1.3×l0^3 km^3, which is ~13 to 20% of the present volume of the mound (Table 1, Fig. S3). It is readily apparent that the volume of the present mound exceeds the volume of sediment from Gale's catchment area mobilized by the contributory fluvial network and overland flow by a factor of 5 or more. Thus, mechanisms other than fluvial transport are needed to explain the remaining 80 to 87% of the mound's sedimentary budget. Previously suggested transportation mechanisms include fluvial, lacustrine, eolian, and polar processes (niveo-eolian), or some combination of the above (e.g., Cabrol et al., 1999; Malin and Edgett, 2000; Irwin et al., 2005; Anderson and Bell, 2010; Milliken et al., 2010; Thomson et al., 2011; Kite et al., 2013). We will return to these options below after considering the topographic implications of these sediment volume estimates. If inferred paleotopography is included, the proportion of the mound moved by water is subject to greater uncertainty, but could be up to 37% (Table S5).

Improved knowledge about the volume of fluvially-transported sediment provides constraints on the maximum elevation where one would expect this material to be found both on and within the mound. As previously noted (e.g., Malin and Edgett, 2000; Irwin et al., 2004; Irwin et al., 2005; Thomson et al., 2011), the mound of Gale rises to an elevation that is almost 3 km higher than the lowest point of the northern rim. Thus, formation of the entire mound in a lacustrine environment would necessitate filling of the northern plains (Fig. 3). There is no evidence of any scour or incision of commensurate scale with this volume of water either into or out of the northern rim of Gale. In this case, we interpret an absence of evidence as evidence of absence, i.e., the lack of a hydrological connection to the northern plains as consistent with such a connection never having formed (Irwin et al., 2004; Irwin et al., 2005). This (non-existent) spillway nevertheless provides a maximum elevation constraint, −2.46 km, above which a lacustrine origin is not tenable. Any putative northern ocean thus would need to either predate Gale, or have a maximum high stand less than approximately −2.46 km; in either case, an ocean could not have contributed to Gale's sediment budget. One factor that contributes to the uncertainty associated with this elevation level is that the northern rim originally may have been slightly higher, although Irwin et al. (2004, 2005) noted that that a north-to-south asymmetry in the crater profile is to be expected given the crater's formation on the regional slope of the dichotomy boundary.

Second, we can also place some constraints on the maximum elevation where one would expect fluvially-transported material to be found *within* the mound. In Fig. 3a, we have tabulated the cumulative volume of material present at or below a given elevation in the mound. Using the present mound topography, the volume of fluvially transported material (~1.3×l0^3 km^3) corrEsponds to an elevation range of−4.21 km to 3.47 km, given choice of assumptions for the mound basal topography (Table S4). This elevation range is about 290 to 1000 m above the base elevation. We therefore propose that fluvial sediments should be located below an elevation of−3.47 km if they constitute mound-forming units (*Curiosity* crossed the −4.21 elevation in September of 2017 (Fig. 3c), and no abrupt transitions were noted). In the paleotopography scenario, the elevation of this lower boundary is estimated to be toward the upper end of this range (−3.7 to −3.3 km; Table S5).

Implications for the origin of the mound

The results help place constraints upon the origin of strata within three zones of the central mound in Gale. Fluvially-transported material could constitute the lower layers of the mound up to an elevation range of−4.21 km to −3.47 km (Fig. 3), consistent with rover observations (e.g., Grotzinger et al., 2015; Fraeman et al., 2016; Hurowitz et al., 2017). One caveat with this elevation constraint is that it assumes the present mound topography; in the paleotopography scenario, the elevation of this lower boundary is estimated to be −3.7 to −3.3 km. For the uppermost 3 km of the mound, a fluvial or lacustrine origin is not consistent as it lies above the northern rim elevation of −2.46 km (Irwin et al., 2004; Irwin et al., 2005). Here, eolian constructional processes are required given the lack of a northern rim breach.

In the intervening ~1 km, i.e., mound material at elevations >−3.47 km and <−2.46 km, it is also likely that the majority of sediment was delivered via the same eolian mechanism responsible for the upper mound. However, water-transported sediments are not precluded in this interval. If fluvial or lacustrine sediments are recognized in this intermediate elevation range (e.g., Dietrich et al., 2013; Le Deit et al., 2013; Fairén et al., 2014; Palucis et al., 2016), this necessitates that additional sources of sediment contributed to the volume of the mound when lakes fed by fluvial and potentially groundwater sources in Gale were operative. For example, wind-blown dust or ash may have contributed some fraction of the sediment during lacustrine phase(s) of evolution, a potential source that is unbounded in this current analysis. Despite these uncertainties, our results suggest that if fluvial or lacustrine deposits are found above an elevation of −3.47 km yet below −2.46 km, they either will be interleaved with other strata or present as mounddraping units that are bounded by basal unconformities depending on if the mound was partially or fully formed at the time of their deposition, respectively.

These results provide specific, testable constraints for the MSL rover. For layers identified via in situ analysis as having a fluvial-delatic or lacustrine origin, both their elevation and their stratigraphic context (i.e., whether they are present as mound-forming or mound-draping units) will help refine the geologic history of sedimentary deposition within Gale. Specifically, these characteristics will provide constraints upon the nature of and relative timing between the fluvial, lacustrine, and eolian processes that have contributed sediment to the Gale mound.

Supplementary Material

Refer to Web version on PubMed Central for supplementary material.

ACKNOWLEDGEMENTS

We greatly appreciate the work of four anonymous reviewers on an earlier version of the manuscript. This work was supported by NASA’s Mars Data Analysis Program (80NSSC17K0647). The raw data for this study are publically available in NASA’s Planetary Data System; the primary source for HRSC data is ESA’s Planetary Science Archive. Individual profile measurements underlying Figure 2 are included in the Supporting Information.

REFERENCES

Anderson RC, and Bell JF III, 2010, Geologic mapping and characterization of Gale Crater and implications for its potential as a Mars Science Laboratory landing site: Mars, v. 5, p. 76–128.

Buhler PB, Fassett CI, Head JW, and Lamb MP, 2014, Timescales of fluvial activity and intermittency in Milna Crater, Mars: Icarus, v. 241, p. 130–147.

Burr DM, Williams RME, Wendell KD, Chojnacki M, and Emery JP, 2010, Inverted fluvial features in the Aeolis/Zephyria Plana region, Mars: Formation mechanism and initial paleodischarge estimates: Journal of Geophysical Research: Planets, v. 115, p. E07011.

Cabrol NA, Grin EA, Newsom HE, Landheim R, and McKay CP, 1999, Hydrogeologic evolution of Gale crater and its relevance to the exobiological exploration of Mars: Icarus, v. 139, no. 2, p. 235–245.

Dietrich WE, Parker T, Sumner DY, Hayes AG, Palucis MC, Williams RME, Calef F, and Team M, 2013, Topographic Evidence for Lakes in Gale Crater, Lunar and Planetary Science Conference, Volume 44: Houston, Texas, Lunar and Planetary Institute, p. abstract #1844.

Edwards CS, Nowicki KJ, Christensen PR, Hill J, Gorelick N, and Murray K, 2011, Mosaicking of global planetary image datasets: 1. Techniques and data processing for Thermal Emission Imaging System (THEMIS) multi-spectral data: Journal of Geophysical Research, v. 116, no. E10008.

Ehlmann BL, and Buz J, 2015, Mineralogy and fluvial history of the watersheds of Gale, Knobel, and Sharp craters: A regional context for the Mars Science Laboratory Curiosity's exploration: Geophysical Research Letters, v. 42, no. 2, p. 264–273.

Fairén AG, et al., 2014, A cold hydrological system in Gale Crater, Mars: Planetary and Space Science, v. 93, p. 101–118.

Fassett CI, and Head JWI, 2005, Fluvial sedimentary deposits on Mars: Ancient deltas in a crater lake in the Nili Fossae region: Geophysical Research Letters, v. 32, p. L14201.

Fedo CM, et al., 2017, Facies Analysis and Basin Architecture of the Upper Part of the Murray Formation, Gale Crater, Mars, Lunar and Planetary Science Conference, Volume 48.

Fergason RL, Lee EM, and Weller L, 2013, THEMIS geodetically controlled mosaics of Mars, Lunar and Planetary Science Conference, Volume 44: Houston, Texas, Lunar and Planetary Institute, p. abstract #1642.

Fraeman AA, Ehlmann BL, Arvidson RE, Edwards CS, Grotzinger JP, Milliken RE, Quinn DP, and Rice MS, 2016, The stratigraphy and evolution of lower Mount Sharp from spectral, morphological, and thermophysical orbital data sets: Journal of Geophysical Research: Planets, v. 121, no. 9, p. 1713–1736. [PubMed: 27867788]

Gabasova LR, and Kite ES, 2018, Compaction and sedimentary basin analysis on Mars: Planetary and Space Science, v. 152, p. 86–106.

Golombek M, et al., 2012, Selection of the Mars Science Laboratory Landing Site: Space Science Reviews, v. 170, p. 641–737.

Golombek MP, et al., 2006, Erosion rates at the Mars Exploration Rover landing sites and long-term climate change on Mars: Journal Geophysical Research, v. 111, no. E12.

Grant JA, Golombek MP, Grotzinger JP, Wilson SA, Watkins MM, Vasavada AR, Griffes JL, and Parker TJ, 2011, The science process for selecting the landing site for the 2011 Mars Science Laboratory: Planetary and Space Science, v. 59, no. 11, p. 1114–1127.

Greeley R, and Guest JE, 1987, Geologic map of the eastern equatorial region of Mars: USGS, U.S. Geol. Surv. Misc. Invest. Ser I-1802-B, scale 1:15,000,000.

Grotzinger JP, et al., 2015, Deposition, exhumation, and paleoclimate of an ancient lake deposit, Gale crater, Mars: Science, v. 350, no. 6257, p. aac7575. [PubMed: 26450214]

Grotzinger JP, et al., 2014, A habitable fluvio-lacustrine environment at Yellowknife Bay, Gale crater, Mars: Science, v. 343, no. 6169, p. 1242777. [PubMed: 24324272]

Harris DR, 1980, Exhumed paleochannels in the Lower Cretaceous Cedar Mountain Formation near Green River, Utah, Brigham Young University, Brigham Young University Geology Studies.

Hurowitz JA, et al., 2017, Redox stratification of an ancient lake in Gale crater, Mars: Science, v. 356, no. 6341, p. eaah6849. [PubMed: 28572336]

Hynek BM, Beach M, and Hoke MRT, 2010, Updated global map of Martian valley networks and implications for climate and hydrologic processes: Journal of Geophysical Research, v. 115, p. 09008.

Hynek BM, and Phillips RJ, 2001, Evidence for extensive denudation of the Martian highlands: Geology, v. 29, no. 5, p. 407–410.

Irwin RP, Howard AD, Craddock RA, and Moore JM, 2005, An intense terminal epoch of widespread fluvial activity on early Mars: 2. Increased runoff and paleolake development: Journal of Geophysical Research, v. 110, p. E12S15.

Irwin RP, Lewis KW, Howard AD, and Grant JA, 2015, Paleohydrology of Eberswalde crater, Mars: Geomorphology, v. 240, p. 83–101.

Irwin RP, Watters TR, Howard AD, and Zimbelman JR, 2004, Sedimentary resurfacing and fretted terrain development along the crustal dichotomy boundary, Aeolis Mensae, Mars: Journal of Geophysical Research, v. 109, p. E09011.

Jolivet M, Barrier L, Dominguez S, Guerit L, Heilbronn G, and Fu B, 2014, Unbalanced sediment budgets in the catchment-alluvial fan system of the Kuitun River (northern Tian Shan, China): Implications for mass-balance estimates, denudation and sedimentation rates in orogenic systems: Geomorphology, v. 214, p. 168–182.

Kite ES, Lewis KW, Lamb MP, Newman CE, and Richardson MI, 2013, Growth and form of the mound in Gale Crater, Mars: Slope wind enhanced erosion and transport: Geology, v. 41, no. 5, p. 543–546.

Le Deit L, Hauber E, Fueten F, Pondrelli M, Rossi AP, and Jaumann R, 2013, Sequence of infilling events in Gale crater, Mars: Results from morphology, stratigraphy, and mineralogy: Journal of Geophysical Research, v. 118, no. 12, p. 2439–2473.

Malin MC, and Edgett KS, 2000, Sedimentary rocks of early Mars: Science, v. 290, no. 5498, p. 1927–1937. [PubMed: 11110654]

Matsubara Y, Howard AD, and Irwin RP III, 2018, Constraints on the Noachian paleoclimate of the Martian highlands from landscape evolution modeling: Journal of Geophysical Research: Planets, v. 123, no. 11, p. 2958–2979.

Milliken RE, Grotzinger JP, and Thomson BJ, 2010, Paleoclimate of Mars as captured by the stratigraphic record in Gale Crater: Geophysical Research Letters, v. 37, p. L04201.

Moore JM, Howard AD, Dietrich WE, and Schenk PM, 2003, Martian layered fluvial deposits: Implications for Noachian climate scenarios: Geophysical Research Letters, v. 30, no. 24.

Neukum G, and Jaumann R, 2004, HRSC: The High Resolution Stereo Camera of Mars Express, *in* Wilson A, ed., Mars Express: The Scientific Payload, Volume ESA Special Publication 1240, p. 17–35.

Pain CF, Clarke JDA, and Thomas M, 2007, Inversion of relief on Mars: Icarus, v. 190, no. 2, p. 478–491.

Palucis MC, et al., 2014, The origin and evolution of the Peace Vallis fan system that drains to the Curiosity landing area, Gale Crater, Mars: Journal of Geophysical Research: Planets, v. 119, no. 4, p. 705–728.

Palucis MC, Dietrich WE, Williams RM, Hayes AG, Parker T, Sumner DY, Mangold N, Lewis K, and Newsom H, 2016, Sequence and relative timing of large lakes in Gale crater (Mars) after the formation of Mount Sharp: Journal of Geophysical Research, v. 121, no. 3, p. 472–496.

Rampe E, et al., 2017, Mineralogy of an ancient lacustrine mudstone succession from the Murray formation, Gale crater, Mars: Earth and Planetary Science Letters, v. 471, p. 172–185.

Smith DE, et al., 1999, The global topography of Mars and implications for surface evolution: Science, v. 284, no. 5419, p. 1495–1503. [PubMed: 10348732]

Strahler AN, 1957, Quantitative analysis of watershed geomorphology: Transactions, American Geophysical Union, v. 38, p. 913–920.

Thomson BJ, et al., 2011, Constraints on the origin and evolution of the layered mound in Gale Crater, Mars using Mars Reconnaissance Orbiter data: Icarus, v. 214, p. 413–432.

Vaniman DT, et al., 2014, Mineralogy of a mudstone at Yellowknife Bay, Gale crater, Mars: Science, v. 343, no. 6169, p. 1243480. [PubMed: 24324271]

Williams RME, et al., 2013, Martian fluvial conglomerates at Gale crater: Science, v. 340, no. 6136, p. 1068–1072. [PubMed: 23723230]

Williams RME, Irwin RP, and Zimbelman JR, 2009, Evaluation of paleohydrologic models for terrestrial inverted channels: Implications for application to martian sinuous ridges: Geomorphology, v. 107, no. 3, p. 300–315.

Williams RME, and Malin MC, 2008, Sub-kilometer fans in Mojave crater, Mars: Icarus, v. 198, no. 2, p. 365–383.

Williams RME, and Phillips RJ, 2001, Morphometric measurements of martian valley networks from Mars Orbiter Laser Altimeter (MOLA) data: Journal of Geophysical Research, v. 106, no. E10, p. 23,737–723,751.

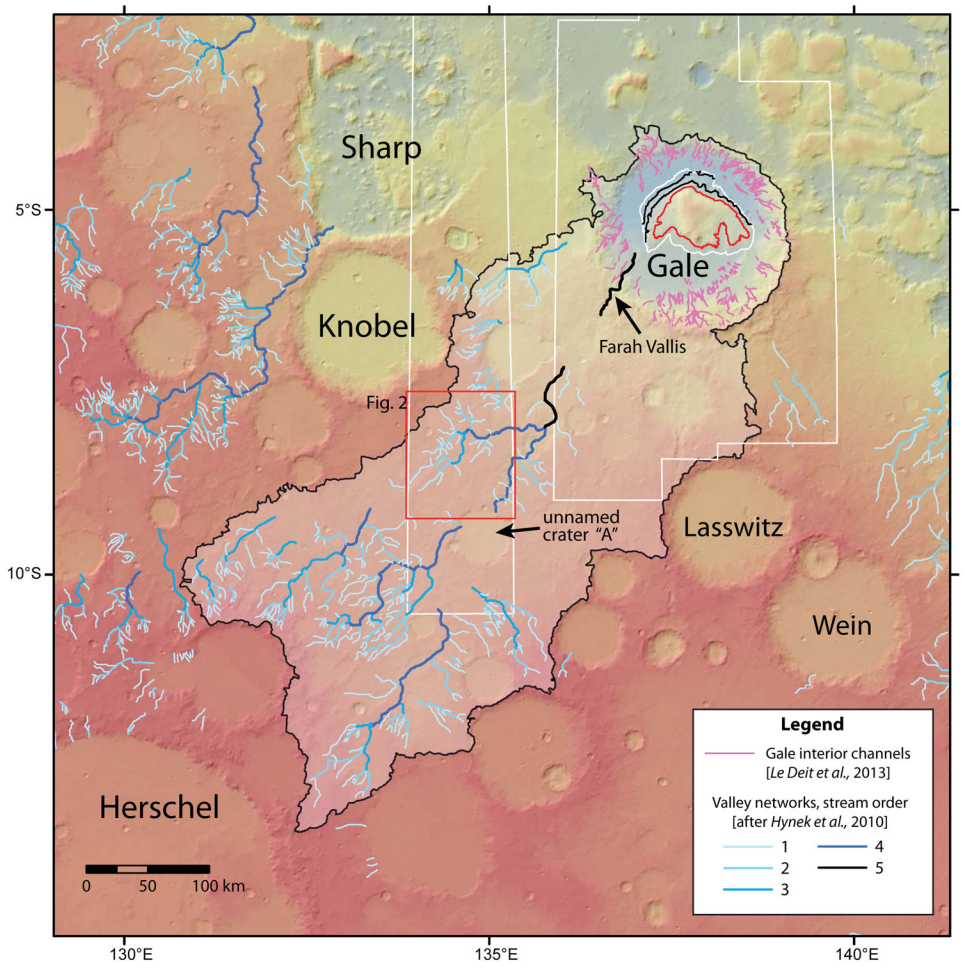

Figure 1.

Shaded relief map of Gale crater region from MOLA topography. Watershed is outlined in black; white boxes give extents of HRSC DEMs. Location of Fig. 2 is outlined in red. Valley networks were modified from Hynek el al. (2010) and are color-coded according to Strahler stream order. Interior channels and inverted channels given in pink were mapped by Le Deit et al. (2013). White line encircles outer boundary of Gale mound and encloses red and black lines that are the contour intervals given in Fig. 3 (−2.46, −3.47, and −4.21 km, respectively).

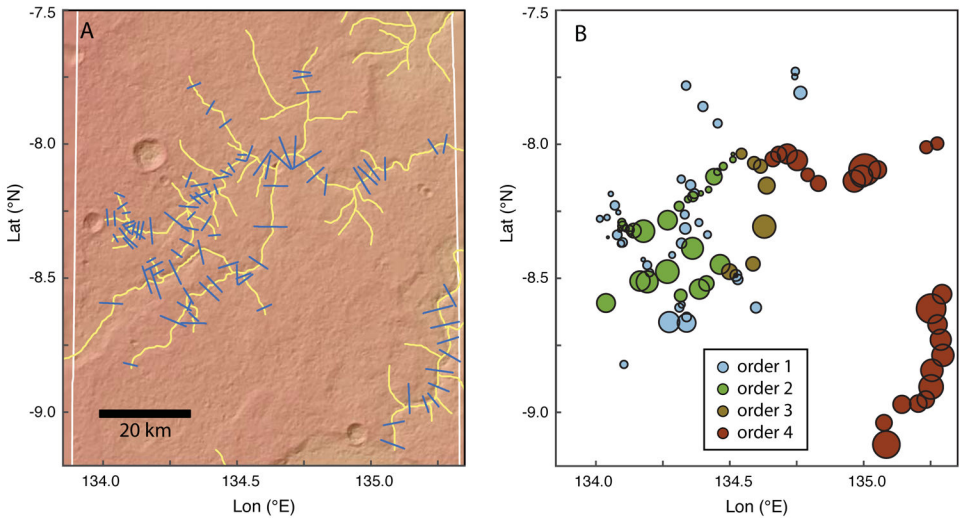

Figure 2.

(a) Mapped valley network locations of 2D-profiles given with blue bars, **(b)** Locations of N=96 profiles from Fig. 2a with points colored according to valley network stream order (1–4) and sized according to relative cross sectional area.

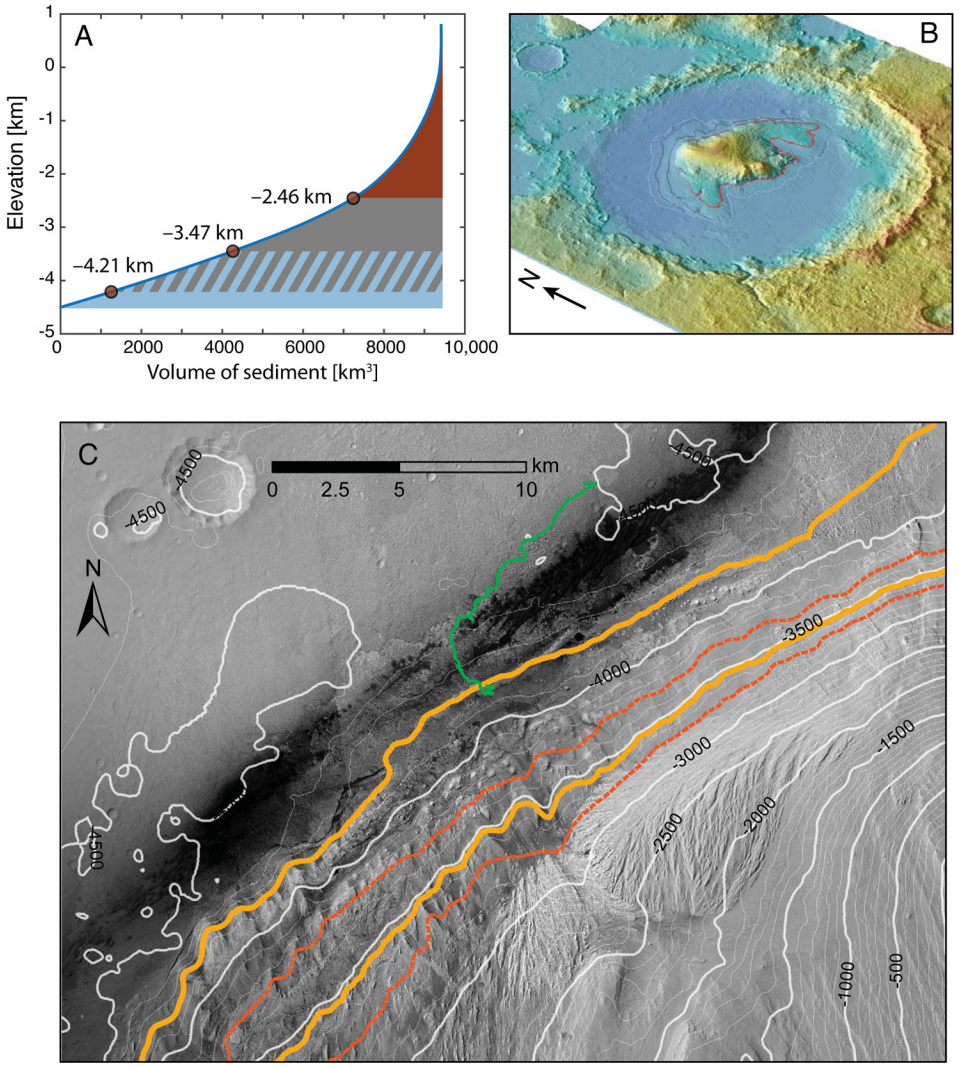

Figure 3.

(a) Cumulative volume of Gale's mound versus elevation. The total mound volume is 9.41 $\times 10^3$ km^3 of sediment above the base elevation of −4.5 km. Lower red circles give range of maximum elevation of mounds if it were built from fluvially-transported sediment (−4.21 km to −3.47 km, region shaded in blue). Upper red circle gives elevation of spillover to north at −2.46 km; region shaded in red. **(b)** Perspective view of Gale crater flooded up to the spillover elevation of −2.46 km. Red contour line is this same elevation of −2.46 km; black contour lines are −3.47 km and −4.21 km, although they are truncated where they intersect the mapped outer boundary of the mound encircled with a white line, **(c)** Countour map of NW portion of Mt. Sharp; contours are from HRSC h1927_0000. MSL traverse from Sols 1–2313 is given with green line. Solid orange contours are the −4.21 km and −3.47 km elevation boundaries based on the current topography; dashed red contours are the −3.7 km and −3.3 km elevation boundaries using inferred paleotopography.

Table 1.

Volume balance components

Volume [km^3]	Source
$2\pm1 \times 10^2$	Interior channels
$8.1\pm13 \times 10^2$	Exterior valley network (inc. Farah Vallis)
$\leq 2.4 \times 10^2$	Overland flow
$9.4\pm0.1 \times 10^3$	Mound volume